JOURNAL OF GUIDANCE, CONTROL, AND DYNAMICS
Vol. 37, No. 4, July–August 2014

Lyapunov-Based Guidance for Orbit Transfers and Rendezvous in Levi-Civita Coordinates

Sonia Hernandez* and Maruthi R. Akella†
University of Texas at Austin, Austin, Texas 78712

DOI: 10.2514/1.62305

This paper considers planar orbit transfers and rendezvous problems around a central body using Lyapunov stability theory. The model used is the Levi-Civita transformation of the planar two-body problem. One of the advantages of working in these transformed coordinates is that the solution to the unperturbed equations of motion is that of a simple harmonic oscillator, so the analytical solution is known at all times during coast phases. We design a closed-loop guidance scheme for orbit transfers from any initial elliptical orbit to any final elliptical orbit using a spacecraft with thrust–coast capabilities. A similar procedure is performed to design a control law for rendezvous with any desired target spacecraft. The proposed Lyapunov functions give rise to asymptotically stabilizing control laws. The algorithms designed are robust to initial and final conditions, computationally fast, and no restrictions are imposed on the magnitude of the thrust. The guidance scheme is also effective in a dynamic model where unmodeled perturbations are present.

Nomenclature

A	=	magnitude of perturbing acceleration
E	=	energy of orbit
e_f	=	difference between the value of a function f and the desired value f^*
$\boldsymbol{F}$	=	perturbing acceleration vector
$\boldsymbol{r}$, r	=	position vector $\in \mathbb{R}^2$ in Cartesian coordinates, position magnitude
$\boldsymbol{u}$	=	position vector $\in \mathbb{R}^2$ in Levi-Civita coordinates
u_1, u_2	=	components of $\boldsymbol{u}$
x, y	=	components of $\boldsymbol{r}$
$\mathcal{W}$	=	frequency of oscillation of analytical unperturbed Levi-Civita solution
α	=	inverse of semimajor axis of the orbit, $1/a$
ϕ	=	control variable

Superscripts

$\cdot$	=	time-derivative in Cartesian coordinates, $\mathrm{d}/\mathrm{d}t$
$\prime$	=	time-derivative in Levi-Civita coordinates, $\mathrm{d}/\mathrm{d}s$
$*$	=	desired final value

I. Introduction

HISTORICALLY, the problem of computing finite thrust orbit transfers and rendezvous has been studied extensively in the literature [1,2]. Much work has concentrated on optimal transfers using both direct and indirect methods [3–7]. However, these solutions are computationally expensive and do not often result in closed-form solutions. Some attention has been given to heuristic models to achieve orbit transfers where feedback control laws are designed based on candidate Lyapunov functions, but these use mostly singular perturbation theory in conjunction with Lagrange's variational equations to establish suitable guidance laws [8–11]. Similar methods to rendezvous a spacecraft with a target have been studied as well [12,13]. In this paper, we take advantage of Lyapunov theory to design guidance laws for closed orbit transfers as well as rendezvous; however, the approach presented is quite novel because not only are there are no additional time-scale-related approximations involved, but the resulting new controllers require significantly lower computation time to permit easy onboard implementation.

We take on a new approach to the problem by working in a transformed model to design Lyapunov-based control laws. The model we use is the classical Levi-Civita regularization transformation of the planar two-body problem [14,15]. The main idea behind regularization is to transform both the position coordinates and time coordinates to a new model. This model has been mostly used in the past to deal with close-encounter-type problems [14,16], but has only been slightly exploited for orbit transfer problems. For example, in [17], this model is used to solve the minimum-time transfer between coplanar circular orbits using Lagrange multipliers. More recently, we have used this model to design guidance laws for orbit transfers from elliptical to circular coplanar orbits [18]. One of the main advantages of working in these transformed coordinates is that the solution to the unperturbed equations of motion is that of a simple linear harmonic oscillator, where the frequency of oscillation is a function of a, the semimajor axis of the orbit. Therefore, during any coast phase, the analytical solution is explicitly characterized. Additionally, this model is advantageous for propagating highly eccentric orbits. This is due to the time transformation, where an orbit segmented into equal time steps becomes segmented equally in position by using this model. Because small time steps present an issue when propagating Keplerian orbits, this transformation is useful to provide better resolution near periapsis.

The major contributions of this paper are twofold: 1) arbitrary planar orbit transfers among closed orbits and 2) planar rendezvous. The orbit transfer problem requires matching three desired parameters: semimajor axis a^*, eccentricity e^*, and argument of periapsis ω^*. The rendezvous problem, on the other hand, requires matching four parameters: two position coordinates $\boldsymbol{r}^*$ and two velocity coordinates $\dot{\boldsymbol{r}}^*$ of the target spacecraft. The idea is to design the control laws by using Lypaunov stability theory. This involves forming a candidate Lyapunov function (i.e., quadratic function) that is always monotonic (i.e., nonincreasing) and minimum at our desired final state. Note that, although the guidance schemes are designed in the transformed regularized coordinates, the results can be explicitly characterized in the original coordinates; the transformation procedure merely acts as an enabler for the design. The algorithms designed are robust to any initial and final conditions, computationally fast, and can be used for both low- and high-thrust problems. Also, the effectiveness of the guidance scheme in a dynamic environment where unmodeled perturbations are present is

Received 6 March 2013; revision received 9 September 2013; accepted for publication 10 September 2013; published online 11 March 2014.

*Graduate Student, Department of Aerospace Engineering and Engineering Mechanics; sonia.hernandez@utexas.edu.

†Associate Professor, Department of Aerospace Engineering and Engineering Mechanics; makella@mail.utexas.edu. Associate Fellow AIAA.

shown via numerical simulation. We show the validity of this by adding J_2 perturbations to an example.

The first problem solved in this paper is to design a closed-loop guidance scheme for a coplanar orbit transfer from any initial closed orbit (with semimajor axis a_0, eccentricity $0 \le e_0 < 1$, and argument of periapsis ω_0) to any final closed orbit with a specified a^*, $0 \le e^* < 1$, and ω^*, using a spacecraft with thrust–coast capabilities. Petropoulos [8] has developed an algorithm using Lyapunov stability to perform noncoplanar orbit transfers using a coast–thrust mechanism, but this algorithm is restricted to low-thrust solutions only. A detailed summary of Lyapunov-like algorithms previously developed is presented in [19], however, these methods typically all require computing the time derivatives associated with Lagrange's planetary equations and are restricted to low-thrust engines. In this paper, the convergence to the desired orbit is performed in two steps. The first step involves converging the spacecraft orbit to the desired semimajor axis a^* by continuously thrusting, even though the eccentricity and orientation at this stage may not be the desired one, by using a Lyapunov analysis that gives rise to an asymptotically stabilizing control law. Once a^* has been reached to within a specified tolerance, the second step of the algorithm involves matching the desired eccentricity and argument of periapsis (while always maintaining the specified target a^*), using exactly the same control law as before, but with an added on/off switching mechanism for coasting during certain intervals. A special case of the transfer problem is also addressed, in which we desire to transfer to a circular orbit ($e^* = 0$). In this case, only two orbital parameters are required to be matched because the argument of periapsis can be left undefined for a circular orbit.

The second problem solved is to design a closed-loop guidance scheme to achieve rendezvous between two coplanar spacecraft that are in bounded orbits; that is, to match both the position and velocity of a target spacecraft orbiting a central body. No restrictions are posed upon the initial position and velocity separations between the chaser and target. The first step in the algorithm involves converging only the chaser's initial semimajor axis to the target's semimajor axis a^*, in fact by using the same control law as in the aforementioned orbit transfer problem. Once a^* has been reached to within a specified tolerance, the second step of the algorithm involves achieving rendezvous by adding an on/off switching mechanism for coasting during certain intervals; however, the control law is the same one that is used to match the semimajor axis. Guidance laws have been developed previously for close proximity and terminal rendezvous problems using Lyapunov theory, for closed-loop feedback control [12,13] as well as adaptive control schemes [20]. However, to our best knowledge, the algorithm presented in this paper is the first noniterative finite thrust control scheme to perform a full rendezvous with a target, without any restriction of the initial location of the chaser.

The paper is organized as follows. We begin Sec. II by deriving the Levi-Civita equations of motion of a spacecraft, which is allowed to thrust in a two-body force model. The next section deals with designing a guidance scheme to target only one orbital parameter: the semimajor axis a^*. This serves as a motivating example to solve both the orbit transfer and rendezvous problems. We are able to show in Sec. IV that, by allowing the spacecraft to have thrust–coast capabilities, we can perform any planar closed-orbit transfer problem. In Sec. V, the guidance scheme necessary to rendezvous with a target spacecraft is established. Several examples are shown for all the problems discussed. The last section summarizes the paper and discusses future work.

II. Equations of Motion in Levi-Civita Coordinates

In this section, the Levi-Civita equations of motion are derived from the governing equations of two bodies. The equations of motion of a spacecraft in a perturbed planar two-body model are

$$\ddot{\boldsymbol{r}} = -\frac{\mu}{r^3}\boldsymbol{r} + \boldsymbol{F} \tag{1}$$

where μ is the gravitational parameter of the central body, the position vector $\boldsymbol{r} = [x \quad y]^T$ has magnitude $r = \sqrt{x^2 + y^2}$, and $\boldsymbol{F}$ is the perturbing acceleration. Using polar coordinates r and θ (where θ is measured counterclockwise from the positive x axis), the position can be written as

$$x = r\cos\theta \quad y = r\sin\theta \tag{2}$$

The main idea behind regularization is to transform both the position coordinates and time coordinates to a new model [14,16,21]. There are three steps to convert Eq. (1) into the regularized model, following the notation in [14].

1) Change position coordinates (Levi-Civita coordinates).
2) Introduce a fictitious time, by means of a velocity transformation.
3) Use conservation of energy.

We begin by introducing the following transformation:

$$\begin{matrix} x = u_1^2 - u_2^2 \\ y = 2u_1u_2 \end{matrix} \Leftrightarrow \begin{matrix} u_1 = \sqrt{r}\cos(\theta/2) \\ u_2 = \sqrt{r}\sin(\theta/2) \end{matrix} \tag{3}$$

where the transformed position vector is $\boldsymbol{u} = [u_1, u_2]^T$. The visual relationship between Eqs. (2) and (3) is shown in Fig. 1. Note,

$$r^2 = x^2 + y^2 \Leftrightarrow r = \boldsymbol{u}\cdot\boldsymbol{u} = u_1^2 + u_2^2 \tag{4}$$

The transformation from $\boldsymbol{u}$ to $\boldsymbol{r}$ can be expressed in terms of the following linear operator:

$$\boldsymbol{r} = \mathcal{L}(\boldsymbol{u})\boldsymbol{u} = \begin{bmatrix} u_1 & -u_2 \\ u_2 & u_1 \end{bmatrix}\begin{bmatrix} u_1 \\ u_2 \end{bmatrix} \tag{5}$$

The linear operator $\mathcal{L}(\boldsymbol{u})$ has the following properties [21]:

1) $\mathcal{L}^T(\boldsymbol{u})\mathcal{L}(\boldsymbol{u}) = r\boldsymbol{I}$, where $\boldsymbol{I}$ is the identity matrix.
2) $\mathcal{L}'(\boldsymbol{u}) = \mathcal{L}(\boldsymbol{u}')$, where $'$ denotes the time derivative.
3) $\mathcal{L}(\boldsymbol{u})\boldsymbol{v} = \mathcal{L}(\boldsymbol{v})\boldsymbol{u}$.
4) $(\boldsymbol{u}\cdot\boldsymbol{u})\mathcal{L}(\boldsymbol{v})\boldsymbol{v} - 2(\boldsymbol{u}\cdot\boldsymbol{v})\mathcal{L}(\boldsymbol{u})\boldsymbol{v} + (\boldsymbol{v}\cdot\boldsymbol{v})\mathcal{L}(\boldsymbol{u})\boldsymbol{u} = \boldsymbol{0}$.

The second step in the derivation involves introducing a velocity transformation

$$\dot{\boldsymbol{r}} = \frac{1}{r}\boldsymbol{r}' \Leftrightarrow \frac{\mathrm{d}\boldsymbol{r}}{\mathrm{d}t} = \frac{1}{r}\frac{\mathrm{d}\boldsymbol{r}}{\mathrm{d}s}$$

Note, that

$$(\dot{\cdot}) = \frac{\mathrm{d}}{\mathrm{d}t}()$$

denotes the time derivative in $\boldsymbol{r}$ coordinates, whereas

$$()' = \frac{\mathrm{d}}{\mathrm{d}s}()$$

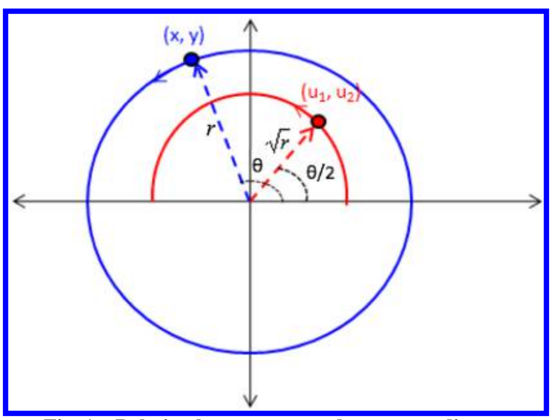

Fig. 1 Relation between x-y and u_1-u_2 coordinates.

is the time derivative in $\boldsymbol{u}$ coordinates:

$$\frac{\mathrm{d}}{\mathrm{d}t} = \frac{1}{r}\frac{\mathrm{d}}{\mathrm{d}s} \tag{6}$$

$$\frac{\mathrm{d}^2}{\mathrm{d}t^2} = \frac{1}{r^2}\frac{\mathrm{d}^2}{\mathrm{d}s^2} - \frac{r'}{r^3}\frac{\mathrm{d}}{\mathrm{d}s} \tag{7}$$

Using properties 2 and 3 of the linear operator $\mathcal{L}(\boldsymbol{u})$, the first- and second-order derivative of $\boldsymbol{r}$ in terms of $\boldsymbol{u}$ coordinates are

$$\boldsymbol{r}' = \frac{\mathrm{d}}{\mathrm{d}s}\boldsymbol{r} = \frac{\mathrm{d}}{\mathrm{d}s}[\mathcal{L}(\boldsymbol{u})\boldsymbol{u}] = 2\mathcal{L}(\boldsymbol{u})\boldsymbol{u}' \tag{8}$$

$$\boldsymbol{r}'' = \frac{\mathrm{d}}{\mathrm{d}s}\boldsymbol{r}' = 2\mathcal{L}(\boldsymbol{u}')\boldsymbol{u}' + 2\mathcal{L}(\boldsymbol{u})\boldsymbol{u}'' \tag{9}$$

Using Eq. (7), the second time derivative of $\boldsymbol{r}$ can be written as

$$\ddot{r} = \frac{1}{r^2}r'' - \frac{r'}{r^3}r'$$

which, when compared with Eq. (1), and solved for $\boldsymbol{r}''$ gives

$$\boldsymbol{r}'' = \frac{1}{r}[r'\boldsymbol{r}' - \mu\boldsymbol{r} + r^3\boldsymbol{F}] \tag{10}$$

Using the fact that $r = \boldsymbol{u}\cdot\boldsymbol{u}$, its time derivative is $r' = 2\boldsymbol{u}\cdot\boldsymbol{u}'$. Equating Eqs. (9) and (10), and using Eqs. (5) and (8),

$$2\mathcal{L}(\boldsymbol{u}')\boldsymbol{u}' + 2(\boldsymbol{u})\boldsymbol{u}'' = \frac{r'}{r}2\mathcal{L}(\boldsymbol{u})\boldsymbol{u}' - \frac{\mu}{r}\mathcal{L}(\boldsymbol{u})\boldsymbol{u} + r^2\boldsymbol{F}$$

Rearranging, and using property 4 of the linear operator $\mathcal{L}(\boldsymbol{u})$,

$$\boldsymbol{u}'' + \frac{\mu/2 - \boldsymbol{u}'\cdot\boldsymbol{u}'}{\boldsymbol{u}\cdot\boldsymbol{u}}\boldsymbol{u} = \frac{1}{2}(\boldsymbol{u}\cdot\boldsymbol{u})\mathcal{L}^T(\boldsymbol{u})\boldsymbol{F} \tag{11}$$

The third and last step in the transformation involves using the conservation of energy principle. Before, note that $\dot{\boldsymbol{r}} = \boldsymbol{r}'/r = 2\mathcal{L}(\boldsymbol{u})\boldsymbol{u}'/r$ and, therefore, the norm of the velocity squared is

$$v^2 = \dot{\boldsymbol{r}}^T\dot{\boldsymbol{r}} = \frac{4}{r}\boldsymbol{u}'\cdot\boldsymbol{u}' \tag{12}$$

where we have made use of property 1 of the linear operator. The energy of the two-body problem

$$E = \frac{v^2}{2} - \frac{\mu}{r} = \frac{1}{r}(2\boldsymbol{u}'\cdot\boldsymbol{u}' - \mu) \tag{13}$$

Note that the fraction in the second term of Eq. (11) is in fact $(\mu/2 - \boldsymbol{u}'\cdot\boldsymbol{u}')/r = -E/2$. Therefore, the Levi-Civita equations of motion are

$$\boldsymbol{u}'' = \frac{E}{2}\boldsymbol{u} + \boldsymbol{F}_u \tag{14}$$

where the perturbing acceleration in Levi-Civita coordinates $\boldsymbol{F}_u = r\mathcal{L}^T(\boldsymbol{u})\boldsymbol{F}/2$. The energy E varies with time according

$$E' = \frac{4}{r}\boldsymbol{u}'\cdot\boldsymbol{F}_u = 2\boldsymbol{u}'\cdot\mathcal{L}^T(\boldsymbol{u})\boldsymbol{F} \tag{15}$$

Lemma 1: The quadratic potential

$$C(s) = -\frac{E}{4}(u_1^2 + u_2^2) + (u_1'^2 + u_2'^2) = \frac{\mu}{2} \tag{16}$$

is an integral of motion of the perturbed equations of motion in Eqs. (14) and (15).

Proof: Taking the time derivative of $C(s)$, and using Eqs. (14) and (15), it is readily seen that $C'(s) = 0$, regardless of the value of the perturbing acceleration $\boldsymbol{F}$ and, in fact, $C(s) = C(s_0) = \mu/2$ $\forall\ s \geq s_0$. □

A. Unperturbed Equations of Motion

In the case when there is no perturbing acceleration acting on the spacecraft, that is, $\boldsymbol{F} = 0$, the equations of motion in Eq. (14) become decoupled linear harmonic oscillators and $E' = 0$ from Eq. (15). The analytical solution is therefore known, with a frequency of oscillation of $\mathcal{W} = \sqrt{-E/2}$. Because, in this case, we are dealing with closed orbits, $E < 0$ and, therefore, its position in s time coordinates is given by

$$\begin{aligned} u_1(s) &= u_{1_0}\cos(\mathcal{W}s) + \frac{u'_{1_0}}{\mathcal{W}}\sin(\mathcal{W}s) = A_{u_1}\cos(\mathcal{W}s + \Phi_{u_1}) \\ u_2(s) &= u_{2_0}\cos(\mathcal{W}s) + \frac{u'_{2_0}}{\mathcal{W}}\sin(\mathcal{W}s) = A_{u_2}\cos(\mathcal{W}s + \Phi_{u_2}) \end{aligned} \tag{17}$$

where

$$A_\xi = \sqrt{u_{1_0}^2 + (u'_{1_0}/\mathcal{W})^2} \quad \text{and} \quad \Phi_{u_1} = \tan^{-1}\left(\frac{u'_{1_0}}{u_{1_0}\mathcal{W}}\right)$$
$$A_\eta = \sqrt{u_{2_0}^2 + (u'_{2_0}/\mathcal{W})^2} \quad \text{and} \quad \Phi_{u_2} = \tan^{-1}\left(\frac{u'_{2_0}}{u_{2_0}\mathcal{W}}\right)$$

and u_{1_0}, u_{2_0}, u'_{1_0}, and u'_{2_0} are the initial conditions at s_0. Note, that in the case when the orbit is unbounded, that is, $E \geq 0$, the analytical solution is also known, and its solution has an exponential form, with its exponents given by the roots of its characteristic equation.

B. Finite Thrust Maneuvers

Suppose that the perturbation now comes from a finite thrust engine, with constant thrust magnitude T, specific impulse c, and variable thrust angle ϕ (measured counterclockwise from the positive x axis), such that

$$\boldsymbol{F} = A\begin{bmatrix}\cos\phi \\ \sin\phi\end{bmatrix}$$

The acceleration magnitude $A = T/m$ and m is the mass of the spacecraft at any point in time, which varies according to $\dot{m} = -T/c$. In the Levi-Civita coordinates, this corresponds to

$$\boldsymbol{F}_u = \frac{Ar^{3/2}}{2}\begin{bmatrix}\cos(\phi - \theta/2) \\ \sin(\phi - \theta/2)\end{bmatrix} \tag{18}$$

For implementation purposes, it is convenient to introduce a new parameter $\alpha = 1/a$, where a is the semimajor axis of the orbit. The parameter α is related to the energy E of an orbit through the relation $E = -\mu/(2a) = -(\mu/2)\alpha$ and its derivative $\alpha' = -(2/\mu)E'$. Combining this into Eqs. (14) and (15) results in the new equations of motion

$$\begin{aligned} \boldsymbol{u}'' &= -\frac{\mu\alpha}{4}\boldsymbol{u} + \frac{Ar^{3/2}}{2}\begin{bmatrix}\cos(\phi - \theta/2) \\ \sin(\phi - \theta/2)\end{bmatrix} \\ \alpha' &= -\frac{4A}{\mu}r^{1/2}\sqrt{u_1'^2 + u_2'^2}\sin(\phi + \lambda - \theta/2) \quad m' = -r\frac{T}{c} \end{aligned} \tag{19}$$

where we have defined

$$\sin\lambda = \frac{u_1'}{\sqrt{u_1'^2 + u_2'^2}} \quad \text{and} \quad \cos\lambda = \frac{u_2'}{\sqrt{u_1'^2 + u_2'^2}}$$

III. Matching Semimajor Axis

As a first step to performing orbit transfers and rendezvous, we will start with a motivating example. Suppose for now that we are interested in matching the semimajor axis of a target orbit, but do not take into account any other orbital elements. Let the semimajor axis of the target orbit be denoted as a^* and, therefore, its inverse is $\alpha^* = 1/a^*$. At any point in time (in s coordinates) the spacecraft, whose motion is governed by Eq. (19), has a semimajor axis $a(s)$, and correspondingly $\alpha(s) = 1/a(s)$. The difference between the current $\alpha(s)$ and the target α^* is denoted by $e_\alpha = \alpha - \alpha^*$.

The quadratic candidate Lyapunov-like function

$$V = \frac{1}{2} e_\alpha^2 \tag{20}$$

is minimized when the semimajor axis of the spacecraft matches that of the desired orbit. The time derivative of V (with respect to the s variable) along solutions of Eq. (19) is given by

$$\begin{aligned} V' &= e_\alpha e_\alpha' = (\alpha - \alpha^*)\alpha' \\ &= -(\alpha - \alpha^*) \frac{4A\sqrt{r}\sqrt{u_1'^2 + u_2'^2}}{\mu} \sin(\phi + \lambda - \theta/2) \end{aligned}$$

Choosing

$$\phi = -\lambda + \theta/2 + \sin^{-1}(K e_\alpha), \qquad K = 1/|e_{\alpha_0}| > 0 \tag{21}$$

where $e_{\alpha_0} = e_\alpha(s_0)$, results in

$$V' = -\frac{4A\sqrt{r(u_1'^2 + u_2'^2)}}{\mu} K e_\alpha^2 \le 0 \tag{22}$$

which ensures that V is nonincreasing.

Proposition 1: Let a spacecraft with a constant available maximum thrust T and initial mass m_0 be on a closed orbit with initial semimajor axis $a(s_0) = a_0$. All solutions governed by the force model (19) with control (21) and $A = T/m$ converge to any prescribed final semimajor axis a^*.

Proof: Because of the commanded thrust protocol for driving $\alpha(s)$ to some prescribed final value α^* [by Eq. (21)], $\alpha(s)$ becomes an exponential function of $e_\alpha(s)$, since

$$e_\alpha' = \alpha' = -K_1 A f(\boldsymbol{u}, \boldsymbol{u}') e_\alpha$$

where $K_1 = (4K)/\mu > 0$ and $f(\boldsymbol{u}(s), \boldsymbol{u}'(s)) = \sqrt{(u_1^2 + u_2^2)(u_1'^2 + u_2'^2)}$. We are guaranteed that $K_1 > 0$ and $A(s) = T/m(s) > 0$ [as long as $m(s) > 0$, otherwise $A = 0$ by turning the thrusters off]. Therefore, to show that we always converge to the desired α^*, it is necessary to show that $f(\boldsymbol{u}, \boldsymbol{u}')$ cannot become zero, and if it does, it cannot stay at zero indefinitely.

The signal $\alpha(s)$ is monotonic due to the control chosen in Eq. (21) [i.e., $\alpha(s)$ is nondecreasing for the case $\alpha^* > \alpha_0$ and $\alpha(s)$ is nonincreasing for the case $\alpha^* < \alpha_0$]. Therefore, we are guaranteed that there exists some $\alpha_{\min}$ and $\alpha_{\max}$ such that $0 < \alpha_{\min} \le \alpha(s) \le \alpha_{\max}$ $\forall\ s \ge s_0$. Specifically, $\alpha_{\min} \doteq \min[\alpha(s_0), \alpha^*]$ and $\alpha_{\max} \doteq \max[\alpha(s_0), \alpha^*]$.

The integral of motion $C(s) = C(s_0) \ne 0\ \forall\ s \ge s_0$ in Eq. (16) and, because it is a quadratic function of $\boldsymbol{u}$ and $\boldsymbol{u}'$, we can guarantee that both $r = (u_1^2 + u_2^2)$ and $(u_1'^2 + u_2'^2)$ cannot both simultaneously be at zero at the same time, which implies that they cannot perpetually stay at zero. Therefore, $f(\boldsymbol{u}, \boldsymbol{u}')$ cannot remain at zero, which means that there exists finite constants $s^* > 0$ and $\delta > 0$ such that

$$\int_s^{s+s^*} f(\boldsymbol{u}(\sigma), \boldsymbol{u}'(\sigma))\,\mathrm{d}\sigma \ge \delta \quad \forall\ s \ge s_0$$

We can then conclude that

$$e_\alpha(s) = e_\alpha(s_0) \exp^{-K_1 \int_{s_0}^{s} A(\sigma) f(\boldsymbol{u}, \boldsymbol{u}')\,\mathrm{d}\sigma} \to 0$$

exponentially. □

It is interesting to note that we can lower bound $f(\boldsymbol{u}, \boldsymbol{u}')$ by rewriting it as $f(\boldsymbol{u}, \boldsymbol{u}') = (rv)/2$. The angular momentum of an orbit $h = rv \cos\gamma$, where γ is the flight-path angle, is an integral of motion of any unperturbed orbit. For a circular orbit, $\gamma = 0$ deg for the entire orbit, so that $h = rv$, therefore, $f(\boldsymbol{u}, \boldsymbol{u}') = h/2$ for a circular orbit. For any elliptical orbit, $0 < \sin\gamma \le 1$ and, therefore, f is lower bounded by $f(\boldsymbol{u}, \boldsymbol{u}') \ge h/2$, which again guarantees exponential convergence of $e_\alpha(s)$.

Because we are guaranteed that $0 < \alpha_{\min} \le \alpha(s) \le \alpha_{\max}$, the eccentricity of the orbit $e(s) < 1\ \forall\ s \ge s_0$, so that the orbit during the transfer will always remain bounded. However, for implementation purposes, especially for high-thrust problems, the eccentricity might get very close to the critical value of making the orbit unstable before the desired semimajor axis has been reached. This issue is dealt with in detail in Sec. IV by ensuring that the eccentricity stays below a certain tolerance at all times.

In Sec. III.A, an upper bound on the time taken by the system to achieve a prescribed error tolerance on the semimajor axis is derived. This is done to give the user a maximum possible transfer time. Sec. III.B follows, by a showing the results of the algorithm to reach a desired semimajor axis.

A. Upper Bound on Total Transfer Time

An upper bound on the total propagation time s_f to arrive at a prescribed semimajor axis error tolerance ϵ_α is outlined here. We achieve the desired tolerance when $\epsilon_\alpha = e_\alpha(s_f) = \alpha(s_f) - \alpha^*$. The procedure involves analytically integrating the time derivative of e_α and solving for time.

Because the control variable in Eq. (21) makes the time derivative e_α' a direct function of e_α, by integrating e_α', its solution over time is given by

$$e_\alpha(s) = e_\alpha(s_0) \exp\left[-K_1 \int_{s_0}^{s} A(\sigma) f[\boldsymbol{u}(\sigma), \boldsymbol{u}'(\sigma)]\,\mathrm{d}\sigma\right] \tag{23}$$

To integrate Eq. (23) and obtain an upper bound on s_f, an upper bound on $A(s)$ and $f[\boldsymbol{u}(s), \boldsymbol{u}'(s)]$ needs to be established.

First, the position can be bounded by $r_{\min} \le r(s) \le r_{\max}$. The upper bound is found by solving for the minimum perigee radius possible, $r_{\min} = (1/\alpha_{\max})(1 - e_{\max})$. Recall $E = -(\mu/2)\alpha$, and so the integral of motion in Eq. (16) is also written as

$$C(s) = \frac{\mu}{2} = \frac{\mu}{8}\alpha(u_1^2 + u_2^2) + (u_1'^2 + u_2'^2) \ge \frac{\mu}{8}\alpha_{\min} r(s) \quad \forall\ s \ge s_0$$

therefore, the upper bound on $r(s)$ is $r_{\max} = 4/\alpha_{\min}$. From the energy equation in Eq. (13), it can be established that $v \ge \sqrt{(2\mu)/r}$. Therefore, the function

$$f(\boldsymbol{u}, \boldsymbol{u}') = \frac{1}{2} rv \ge \sqrt{(r\mu)/2} \ge \sqrt{(r_{\min}\mu)/2}$$

and the parameter $A(s) = T/m(s) \ge T/m_0\ \forall\ s \ge s_0$. With these two bounds and given a desired converged tolerance for α^*, $|e_\alpha(s_f)| = \epsilon_\alpha$, Eq. (23) can be integrated to find

$$s_f \le s_0 + \frac{m_0}{KT}\sqrt{\frac{2}{r_{\min}\mu}}[\ln[e_\alpha(s_0)] - \ln(\epsilon_\alpha)] \tag{24}$$

In fact, an even tighter bound can be found on s_f by noting that the mass varies according to $m' = -(T/c)r$. By integrating,

$$m(s) = m_0 - \frac{T}{c}\int_{s_0}^{s} r(\sigma)\,\mathrm{d}\sigma \quad \le m_0 - \frac{T}{c} r_{\min}(s - s_0)$$

Using this fact to integrate e'_α in Eq. (23) yields

$$s_f \leq \frac{1}{K_2}\left[\exp\left(\frac{K_1}{K_2}[\ln[e_\alpha(s_0)] - \ln(\epsilon_\alpha)]\right) - m_0\right] \tag{25}$$

where $K_1 = TK\sqrt{(\mu r_{\min})/2}$ and $K_2 = -(T/c)r_{\min}$. This is a powerful result because it ensures that the transfer time will never take longer than the result in Eq. (25); this is in spite of the fact that our analysis is predominantly asymptotic in nature.

A similar approach can be taken to find a lower bound on the total fuel mass $m(s_f)$ by integrating m' with a bound on $r(s) \leq r_{\max}$, but due to the extreme conservatism inherent with the bounding process, the utility of these estimates is not immediately obvious.

B. Example

An example trajectory under the gravitational pull of Earth ($\mu = 398{,}600\ \mathrm{km^3/s^2}$) using the control in Eq. (21), $T = 200$ N, and $I_{\mathrm{sp}} = 400$ s is shown in Fig. 2. A desired final semimajor axis $a^* = 10{,}000$ km is targeted from an initial circular orbit with $a_0 = 7000$ km. The integration of Eq. (19) is performed in dimensionless units, to avoid buildup numerical errors caused by $e_\alpha = \alpha - \alpha^*$, which can be a very small number when working in units of kilometers. The dimensionless units are distance unit $\mathrm{DU} = a^* = 10{,}000$ km, mass unit $\mathrm{MU} = m_0 = 1000$ kg, and time unit TU, chosen such that $\mu = 1\ \mathrm{DU^3/TU^2}$. The trajectory in x, y coordinates is shown in Fig. 2a, which has been transformed using Eq. (5) from the u_1, u_2 results of the integration. The total transfer time is 4.36 h, whereas using Eq. (25), a bound was found of 7.23 h. Note that the semimajor axis has been met to within 1 km precision, which corresponds to $\epsilon_\alpha = 10^{-4}$, but this has resulted in the final eccentricity reaching a value $e_f = 0.307$. This leads to the next section, which deals on how to target any desired orbit.

IV. Orbit Transfer Problem

As a motivation example, Sec. III dealt with a simple problem, in which a desired semimajor axis was the only parameter targeted. We now deal with a more complex and realistic problem, in which we are interested in performing an orbit transfer to any bounded orbit. We being in Sec. IV.A outlining the theory to perform an orbit transfer to any desired circular orbit and continue in Sec. IV.B by explaining the general orbit transfer to any elliptical orbit, with any relative orientation. For both cases, the algorithm is performed in two steps: first, a matching of the desired semimajor axis a^* by a constant thrust, followed by a matching of the remaining desired orbital elements, by means of a thrust/coast protocol. The beauty of the full designed algorithm is that the control law is exactly the same for both steps. However, one of the reasons for matching the semimajor axis first is because, when the transformation to the Levi-Civita model is performed, a very nice and compact dynamic equation for the time evolution of α' is obtained, which facilitates enormously the derivation of the guidance law (see Sec. III).

A. Elliptical-to-Circular Orbit Transfer

An orbit transfer to any circular orbit requires matching two orbital parameters: semimajor axis and eccentricity. The process of matching the semimajor axis has been explained in the preceding section. To target a specified eccentricity $e^* = 0$ from any initial orbit with $0 \leq e_0 < 1$, the first step is to express the eccentricity in the Levi-Civita coordinates.

The angular momentum vector expressed in the direction $\hat{\boldsymbol{k}}$ normal to the orbit plane is $\boldsymbol{h} = \boldsymbol{r} \times \boldsymbol{v} = (x\dot{y} - y\dot{x})\hat{\boldsymbol{k}}$ and its magnitude

$$\begin{aligned} h = \|\boldsymbol{h}\| &= \begin{bmatrix} x \\ y \end{bmatrix}^T \begin{bmatrix} 0 & 1 \\ -1 & 0 \end{bmatrix}\begin{bmatrix} \dot{x} \\ \dot{y} \end{bmatrix} \\ &= [\mathcal{L}(\boldsymbol{u})\boldsymbol{u}]^T \begin{bmatrix} 0 & 1 \\ -1 & 0 \end{bmatrix}\left[\frac{2}{r}\mathcal{L}(\boldsymbol{u})\boldsymbol{u}'\right] = 2(u_1 u_2' - u_2 u_1') \end{aligned} \tag{26}$$

Recall that $\alpha = 1/a$ and the semilatus rectum $p = a(1 - e^2) = h^2/\mu$. Therefore, the eccentricity can be written as

$$e^2 = 1 - \frac{\alpha}{\mu}h^2 = 1 - 4\frac{\alpha}{\mu}(u_1 u_2' - u_2 u_1')^2 \tag{27}$$

The difference between the current eccentricity $e(s)$ and the desired one e^* is denoted by $e_e = e(s) - e^*$. The quadratic candidate Lyapunov-like function

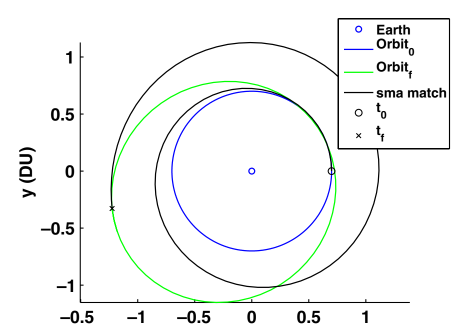

a) Position *x* vs *y*

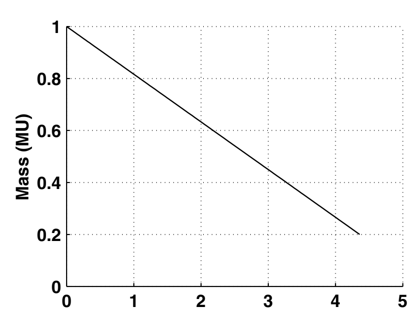

b) Mass *m* vs time

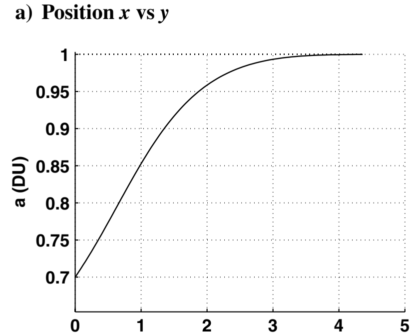

c) Semimajor axis *a* vs time

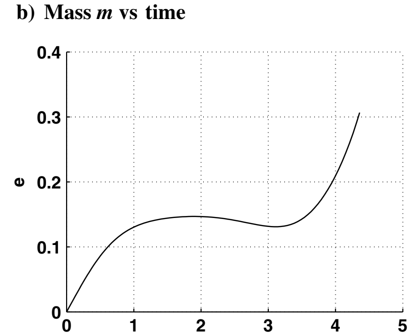

d) Eccentricity *e* vs time

Fig. 2 Semimajor axis matching using control (21), where DU = 10,000 km and MU = 1000 kg.

$$W = V + W_1$$

where V is given by Eq. (20) and

$$W_1 = \frac{1}{2}e_e^2 = \left[\frac{1}{2} - 2\frac{\alpha}{\mu}(u_1u_2' - u_2u_1')^2\right] \tag{28}$$

is minimized when the spacecraft is in a circular orbit, $e^* = 0$ and has the desired semimajor axis a^*. The time derivative in s coordinates of W_1 along solutions of Eq. (19) is given by

$$\begin{aligned} W_1' &= ee' \\ &= -2\frac{\alpha'}{\mu}(u_1u_2' - u_2u_1')^2 - 4\frac{\alpha}{\mu}(u_1u_2' - u_2u_1')[u_1u_2'' - u_2u_1''] \\ &= -\alpha'\frac{h^2}{2\mu} - \frac{h\alpha}{\mu}Ar^{3/2}[u_1\sin(\phi - \theta/2) - u_2\cos(\phi - \theta/2)] \end{aligned}$$

Assume that a spacecraft in an initial orbit with semimajor axis a_0 and eccentricity $0 \leq e_0 < 1$ thrusts using the guidance scheme (21) from $0 \leq s \leq s_i$ until it reaches a desired semimajor axis $\alpha(s_i) \approx \alpha^*$ (to within a specified tolerance ϵ_α), but the eccentricity $e(s_i) \neq e^*$. At this point, the second part of the orbit transfer begins, from $s_i \leq s \leq s_f$, where the quadratic potential W_1 in Eq. (29) is again minimized when $e(s_f) = e^* = 0$. In our definition, convergence on eccentricity is met when $e_e = |e - e^*| \leq \epsilon_e$, Choosing the same control law as in Eq. (21), and since $e_\alpha \approx 0$,

$$\phi = -\lambda + \theta/2 + \sin^{-1}(Ke_\alpha) \approx -\lambda + \theta/2$$

The time derivative of W_1 with control (21) is

$$\begin{aligned} W_1' &= \frac{2AKh^2}{\mu^2}\sqrt{r(u_1'^2 + u_2'^2)}(\alpha - \alpha^*) \\ &+ \frac{Ah\alpha r^{3/2}}{\mu\sqrt{u_1'^2 + u_2'^2}}[u_1u_1' + u_2u_2'] \approx \frac{Ah\alpha r^{3/2}}{\mu\sqrt{u_1'^2 + u_2'^2}}[u_1u_1' + u_2u_2'] \end{aligned} \tag{29}$$

W_1' is regulated to ensure that W_1 is nonincreasing by choosing

$$S_1 = (u_1u_1' + u_2u_2') < 0 \tag{30}$$

The orbit transfer is performed in the following way:

1) Semi-Major Axis Matching from $s_0 \leq s \leq s_i$:

$$A(s) = +T/m \quad \text{while } |\alpha(s) - \alpha^*| > \epsilon_\alpha \tag{31}$$

2) Eccentricity Matching from $s_i \leq s \leq s_f$:

$$A(s) = \begin{cases} +T/m & \text{if } \mathrm{S}_1 < 0 \\ 0 & \text{otherwise} \end{cases} \quad \text{while } |e(s) - e^*| > \epsilon_e \tag{32}$$

Note, that the approximation of $\phi \approx -\lambda + \theta/2$ is used only to define the switching function S_1, which determines when to thrust or coast. However, in the algorithm, the full expression for ϕ, defined in Eq. (21), is used. This ensures not only that $W_1' \leq 0$, but in fact $W' \leq 0$, and so α will also get closer to the desired α^* even during the eccentricity matching section.

In some cases, S_1 can be small in magnitude, and, because of the approximation that $e_\alpha \approx 0$, importance still needs to be given to W_1' [before the approximation was made in Eq. (29)]. When transferring to an orbit with a lower semimajor axis than the initial one, $(\alpha - \alpha^*) \leq 0 \;\forall\; s \geq s_0$; therefore, we ensure $W_1' < 0$ as long as $S_1 < 0$. However, when transferring to a higher semimajor axis, $(\alpha - \alpha^*) \geq 0$, and so it is necessary to ensure that the first term in W_1' never becomes larger in magnitude than the second one, which is ensured as long as

$$\alpha - \alpha^* > \frac{2r}{2 - r\alpha}|S_1|, \quad \text{when } S_1 < 0$$

Also, when performing the semimajor axis matching, especially if using a high enough thrust, the eccentricity might become large enough to where the orbit is unbounded. This can be dealt with by adding a check point, where, during the semimajor axis matching section, the eccentricity is not allowed to get larger than a specified $e_{\max} < 1$. If at some point in time $s = s_{\text{temp}}$, the eccentricity $e(s_{\text{temp}}) = e_{\max}$, the second part of the algorithm will circularize the orbit by temporarily freezing the desired semimajor axis term to $\alpha^* = \alpha(s_{\text{temp}})$. Once the orbit has been circularized ($e \approx 0$), the scheme in Eqs. (31) and (32) can be restarted again, until the desired convergence is met in both α^* and e^*.

Proposition 2: Let a spacecraft with a constant available maximum thrust T and initial mass m_0 be on a closed orbit with a semimajor axis a_0 and an eccentricity $0 \leq e_0 < 1$. All solutions governed by the force model (19) with control (21) and switching algorithm (31) and (32), with a specified $e_{\max}$ constraint, converge to a final circular orbit with semimajor axis a^* and eccentricity $e^* = 0$.

Proof: The first part of the algorithm involves matching a desired semimajor axis, which occurs once $\alpha(s_i) \approx \alpha^*$. This has been proven in Proposition 1. The eccentricity convergence occurs because the quadratic potential in Eq. (29) is radially unbounded, decrescent, and its time derivative $W_1' \leq 0$ by the choice of control ϕ and switching scheme (32). The proof is based on the fact that, due to the thrust protocol, W_1 becomes a convergent sequence, which will inevitably make $e_e \to 0$ as time progresses.

Suppose $S_1(s) < 0 \;\forall s \geq s_i$. In this case, $W_1' < 0 \;\forall s \geq s_0$, which leads to $W_1 \to 0$ as $s \to \infty$. For our convergence definition, this is met at a finite value s_f when $e_e(s_f) \leq \epsilon_e$. Suppose, on the other hand, that $S_1(s) > 0$ for some $s_i \leq s < s_1$, in which case, thrusting is turned off by choosing $A = 0$ and the analytical solution is given by the sinusoidal function in Eq. (17), with a frequency of oscillation $\mathcal{W} = \sqrt{(\mu\alpha^*)/4}$. The function S_1, which is a product of the analytical position and velocity solutions, also becomes a sinusoidal function, and so it cannot remain above zero for an indefinite amount of time (in fact, this amount of time has been computed and is given in the Appendix). During this process, the potential function $W_1(s_i) = W_1(s_1)$ because $W_1' = 0$. When $S(s_1) < 0$, the thruster is turned back on by $A = T/m$, until S_1 crosses the origin again at time s_2, at which point $W_1(s_2) < W_1(s_1)$. The coast/thrust process is repeated again as many times as necessary to reach the desired convergence tolerance ϵ_e; therefore, $W_1(s_i) = W_1(s_1) > W_1(s_2) = W_1(s_3) > W_1(s_4) \gg W_1(s_f) = \frac{1}{2}\epsilon_e^2$. □

It is interesting to note that a different guidance law can be designed to match both the semimajor axis a^* and eccentricity e^* in just one step, rather than in two steps as is designed here. This can be achieved by coupling the candidate Lyapunov functions for both the semimajor axis and eccentricity, $W = V + W_1$, and designing the control law ϕ to make $W' \leq 0$. Even though this solution might give more feasible results in terms of fuel, we have designed the guidance scheme in two steps because we are able to use the *same* control law that matches the semimajor axis to match any circular orbit (or even to match any general orbit, as will be shown in the next subsection).

The orbital parameters of the example transfer shown in Fig. 3 are given in Table 1. The convergence is performed using the guidance scheme (21) and switching function (31) and (32). The initial spacecraft mass is $m_0 = 1000$ kg, the engine parameters are $T = 10$ N and $I_{\text{sp}} = 3000$ s. The results have been scaled using $\text{DU} = a^*$ and $\text{MU} = m_0$. The transfer takes 9.72 days and consumes 193 kg of its mass in fuel (Fig. 3e). Note that the tolerance at which the semimajor axis matching is stopped is $\epsilon_\alpha = 0.1$, at which point it is clear that $a \neq a^*$; however, during the eccentricity matching, the semimajor axis continues to converge to the desired value, due to the fact that the exact same guidance control is used for this section. The time history of the thrust direction is shown in Fig. 3b: It is tangential to the velocity during the first part of the transfer and becomes perpendicular to the velocity as the orbit becomes circularized. The switching function S_1 in Eq. (30) is shown in Fig. 3f beginning at time $t = 4.94$ days, once the eccentricity matching portion begins. Note

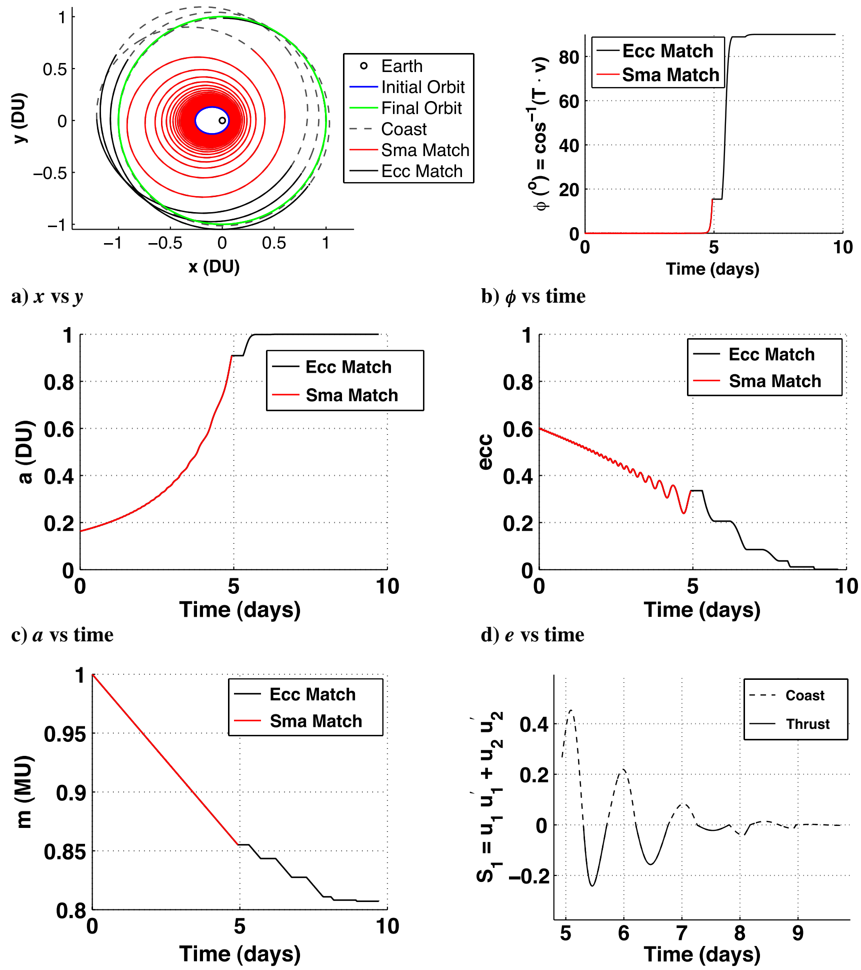

a) x vs y

b) ϕ vs time

c) a vs time

d) e vs time

e) m vs time

f) S_1 vs time during e match

Fig. 3 Eccentricity (Ecc) matching using control (21) and the switching scheme (31) and (32), with parameters in Table 1.

that, at this time, $S_1 > 0$ and, therefore, a coasting phase begins. Around day 8 of the transfer, the switching function S_1 gets close to zero and its time derivative becomes small. When this occurs, it is convenient to coast (even if $S_1 < 0$), until S_1 reaches a minimum, at which point the thrust is turned back on. This is done to avoid chattering and is explained in full detail in Sec. V.

Another low-thrust solution is shown in Fig. 4. In this case, the simulation is a circle-to-circle transfer from $a_0 = 6978$ km to $a_f = 42,164$ km using $T = 1$ N and $I_{sp} = 3000$ s. In this guidance solution, the only required control is to match the desired semimajor axis, because the thrust is low and the eccentricity stays small throughout the transfer. This solution is compared with Edelbaum's optimal analytical solution for circle-to-circle transfers [22], which is derived assuming a constant acceleration magnitude and a low eccentricity ($e \ll 0.1$) during the transfer. The comparison is shown in Table 2. We also use our algorithm in this example to show that a perturbed model due to J_2 [23] is still robust (see comparison in Table 2). As expected, the perturbed model takes longer and uses more propellant; however, because the control law is updated based on the current state, it still converges to the desired orbit.

Table 1 Initial and final orbital parameters for the example in Fig. 3

	Initial orbit	Final orbit
Semimajor axis, km	6878	42,164
Eccentricity	0.6	0.0
Mass, kg	1000	807.1
Time Of Flight, days	— —	9.72

B. Elliptical-to-Elliptical Orbit Transfer

In this section, we discuss the process to target any desired elliptical orbit, with a specified semimajor axis a^*, eccentricity $0 \leq e^* < 1$, and argument of periapsis (AOP) w^*. Without loss of generality, targeting these three orbital elements is equivalent to targeting a^* and the two components of the eccentricity vector $\boldsymbol{e}^* = [e_x^*, e_y^*]^T$.

The eccentricity vector [24] in Levi-Civita coordinates is given by

$$\begin{aligned}\boldsymbol{e} &= \frac{1}{\mu}\left[\left(v^2 - \frac{\mu}{r}\right)\boldsymbol{r} - (\boldsymbol{r}\cdot\boldsymbol{v})\boldsymbol{v}\right]\\ &= \frac{1}{\mu r}[(4\boldsymbol{u}'\cdot\boldsymbol{u}' - \mu)\mathcal{L}(\boldsymbol{u})\boldsymbol{u} - 4(\boldsymbol{u}\cdot\boldsymbol{u}')\mathcal{L}(\boldsymbol{u})\boldsymbol{u}'] \end{aligned} \tag{33}$$

which can be simplified even further by components to

$$e_x = \frac{1}{r}\left[\frac{4}{\mu}(u_1^2 u_2'^2 - u_2^2 u_1'^2) - (u_1^2 - u_2^2)\right] \tag{34}$$

$$e_y = -\alpha u_1 u_2 - \frac{4}{\mu} u_1' u_2' \tag{35}$$

Their respective time derivatives can be algebraically found to be (after extensive simplification)

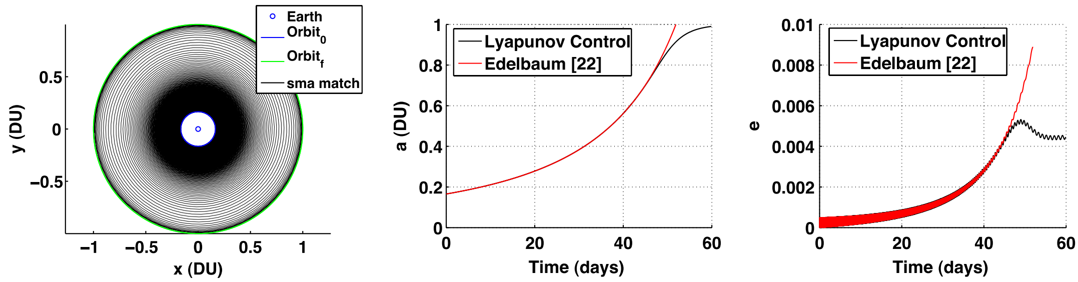

a) Trajectory *x* vs *y* b) Semimajor axis *a* vs time c) Eccentricity *e* vs time

Fig. 4 Comparison of algorithm using control (21) with Edelbaum's analytical low-thrust optimal solution [22].

$$e'_x = \frac{4A\sqrt{r(u_1'^2 + u_2'^2)}}{\mu}[u_1^2 \sin(\phi + \lambda - \theta/2) - r \sin\lambda \cos(\phi - \theta/2)] \tag{36}$$

$$e'_y = \frac{2A\sqrt{r(u_1'^2 + u_2'^2)}}{\mu}[2u_1 u_2 \sin(\phi + \lambda - \theta/2) - r \cos(\phi - \lambda - \theta/2)] \tag{37}$$

The quadratic potential $W = V + W_2$, where V is given by Eq. (20) and

$$W_2 = \frac{1}{2}(\boldsymbol{e} - \boldsymbol{e}^*)^T(\boldsymbol{e} - \boldsymbol{e}^*) \tag{38}$$

is minimized when the semimajor axis and both components of the eccentricity vector are matched. In our definition, convergence on eccentricity is met when

$$e_{e_x} = |e_x - e_x^*| \le \epsilon_e \quad \text{and} \quad e_{e_y} = |e_y - e_y^*| \le \epsilon_e$$

Again, assume that the semimajor axis matching portion occurs from $s_0 \le s \le s_i$ until $e_\alpha = |\alpha(s_i) - \alpha^*| \le \epsilon_\alpha$, specified by the user. Choosing the same control law as in Eq. (21), and since $(\alpha - \alpha^*) \approx 0$,

$$\phi = -\lambda + \theta/2 + \sin^{-1}(K e_\alpha) \approx -\lambda + \theta/2$$

The time derivative of the Lyapunov-like function W_2 is

$$\begin{aligned} W_2' &= e_x'(e_x - e_x^*) + e_y'(e_y - e_y^*) \\ &= \frac{2Ar^{1/2}\sqrt{u_1'^2 + u_2'^2}}{\mu}\left[2Ku_1(u_1 e_{e_x} + u_2 e_{e_y})e_\alpha - \frac{r}{u_1'^2 + u_2'^2}(2u_1'u_2'e_{e_x} + (u_2' - u_1'^2)e_{e_y})\right] \\ &\approx -\frac{2Ar^{3/2}}{\mu\sqrt{u_1'^2 + u_2'^2}}[2u_1'u_2'e_{e_x} + (u_2'^2 - u_1'^2)e_{e_y}] \end{aligned} \tag{39}$$

The convergence to the desired e_x^* and e_y^* to ensure $W_2' \le 0$ is performed by thrusting with an acceleration magnitude $A = T/m$ when

$$S_2 = 2(e_x - e_x^*)u_1'u_2' + (e_y - e_y^*)(u_2'^2 - u_1'^2) > 0 \tag{40}$$

The full orbit transfer is performed in the following way:

1) Semimajor Axis Matching from $s_0 \le s \le s_i$:

$$A(s) = +T/m \quad \text{while } |\alpha(s) - \alpha^*| > \epsilon_\alpha \tag{41}$$

2) Eccentricity and AOP Matching from $s_i \le s \le s_f$:

$$A(s) = \begin{cases} +T/m & \text{if } S_2 > 0 \\ 0 & \text{otherwise} \end{cases} \tag{42}$$

The same $e_{\max}$ constraint is placed on this algorithm, as was done in Sec. IV.A, to ensure that the orbit does not become unbounded.

Proposition 3: Let a spacecraft with a constant available maximum thrust T and initial mass m_0 be on a closed orbit with a semimajor axis a_0, eccentricity $0 \le e_0 < 1$, and argument of periapsis ω_0. All solutions governed by the force model (19) with control (21) and switching function (41) and (42), with an $e_{\max}$ constraint, converge to a final orbit with semimajor axis a^*, eccentricity $0 \le e^* < 1$, and argument of periapsis ω^*.

Proof: The proof follows identically as in Proposition 2, the only difference being that the switching scheme is now given by S_2 in Eq. (40), and the coast time is again analytically solved for in the Appendix. □

An example orbit transfer about Earth is shown in Fig. 5 using control (21) and the switching scheme (41) and (42), with $T = 50$ N, $I_{sp} = 1000$ s s, and initial and final orbital parameters given by Table 3. The results have been scaled using DU $= a^*$ and MU $= m_0 = 1000$ kg. The trajectory in *x-y* coordinates is shown in Fig. 5a, which has been transformed using Eq. (5) from the $\boldsymbol{u}$ results of the integration (shown in Fig. 5b). The time history of the thrust direction is shown in Fig. 5c: It is tangential to the velocity during the first part of the transfer and becomes perpendicular to the velocity as convergence to the desired orbit is achieved. The semimajor axis a, eccentricity e, and argument of periapsis ω over time are shown in Figs. 5f–5h.

To emphasize the different coasting/thrusting phases, a plot of the switching function S_2 in Eq. (40) over time is shown, beginning at the time when the eccentricity (Ecc) and AOP matching section begins. Notice that, as the orbital parameters converge closer to the desired ones, $S_2 \to 0$, and careful attention needs to be given to when to thrust or coast. The assumption was made that $e_\alpha \approx 0$; however, as S_2 becomes smaller in magnitude, the approximation in Eq. (39) might not be not valid anymore to ensure $W_2' < 0$ during the thrusting phase. Therefore, once $|S_2| \le \epsilon$, it is necessary to ensure that thrusting happens only when the bracketed term before the approximation was made in W_2' is negative.

Table 2 Comparison of a low-thrust solution orbit transfer with results shown in Fig. 4

	Transfer time, days	Propellant mass used, kg	Final eccentricity
Edelbaum [22] (unperturbed)	51.89	141.34	0.0091
Lyapunov (unperturbed)	57.47	168.70	0.0048
Lyapunov (J_2 perturbation)	57.49	168.90	0.0050

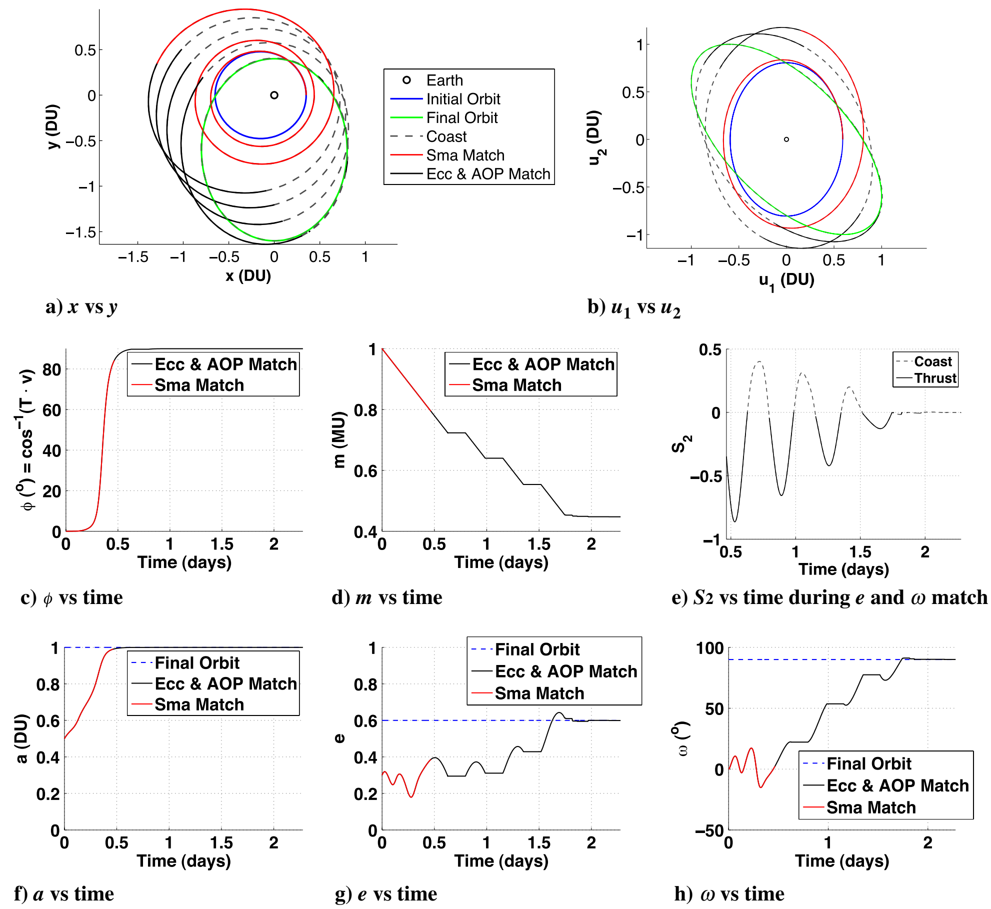

Fig. 5 Orbit transfer using control (21) and the switching scheme (41) and (42), with parameters in Table 3.

V. Rendezvous

This section deals with how to achieve rendezvous with a target spacecraft, that is, to converge to its same position and velocity at the same time. No restrictions are placed on the initial separation between the chaser and the target. We define the candidate Lyapunov function to minimize the error difference in both position and velocity between the chaser and the target

$$
\begin{aligned}
Z &= \frac{\mu}{2}\alpha^* \boldsymbol{e}_{\boldsymbol{u}}^T \boldsymbol{e}_{\boldsymbol{u}} + 2\boldsymbol{e}_{\boldsymbol{u}'}^T \boldsymbol{e}_{\boldsymbol{u}'} \\
&= \frac{\mu}{2}\alpha^*(e_{u_1}^2 + e_{u_2}^2) + 2(e_{u_1'}^2 + e_{u_2'}^2)
\end{aligned} \tag{43}
$$

where the target parameter $\alpha^* = 1/a^*$, and the errors in position and velocity are defined as

$$
\boldsymbol{e}_{\boldsymbol{u}} = \boldsymbol{u} - \boldsymbol{u}^* \quad \boldsymbol{e}_{\boldsymbol{u}'} = \boldsymbol{u}' - \boldsymbol{u}'^* \tag{44}
$$

where the target's state is $\boldsymbol{u}^* = [u_1^*, u_2^*]$ and $\boldsymbol{u}'^* = [u_1'^*, u_2'^*]$. Note Eq. (43) is in fact a measure of the total energy for the harmonic oscillator describing the target's trajectory expressed in the Levi-Civita coordinates.

Table 3 Initial and final orbital parameters for the example in Fig. 5

	Initial orbit	Final orbit
Semimajor axis, km	10,000	20,000
Eccentricity	0.3	0.6
AOP, deg	0.0	90.0
Mass (kg)	1,000	447.4
Time Of Flight (days)	— —	2.28

The time derivative (in s coordinates) of Z is

$$
\begin{aligned}
Z' &= \mu\alpha^* \boldsymbol{e}_{\boldsymbol{u}}^T \boldsymbol{e}_{\boldsymbol{u}'} + 4\boldsymbol{e}_{\boldsymbol{u}'}^T \boldsymbol{e}_{\boldsymbol{u}''} = \mu\alpha^*(e_{u_1}e_{u_1'} + e_{u_2}e_{u_2'}) \\
&\quad + 4e_{u_1'}\left[-\frac{\mu}{4}\alpha^* e_{u_1} - \frac{\mu}{4}e_\alpha u_1 + \frac{Ar^{3/2}}{2}\cos(\phi - \theta/2)\right] \\
&\quad + 4e_{u_2'}\left[-\frac{\mu}{4}\alpha^* e_{u_2} - \frac{\mu}{4}e_\alpha u_2 + \frac{Ar^{3/2}}{2}\sin(\phi - \theta/2)\right] \\
&= -\mu e_\alpha(e_{u_1'}u_1 + e_{u_2'}u_2) \\
&\quad + 2Ar^{3/2}[e_{u_1'}\cos(\phi - \theta/2) + e_{u_2'}\sin(\phi - \theta/2)]
\end{aligned} \tag{45}
$$

If we assume that the semimajor axis of the chaser has been previously matched to be that of the target (to within some specified tolerance) by using the control in Eq. (21), $e_\alpha = \alpha - \alpha^* \approx 0$. Choosing this same control law, $\phi \approx -\lambda + \theta/2$, the time derivative of the potential becomes

$$
\begin{aligned}
Z' &= -\mu e_\alpha \boldsymbol{e}_{\boldsymbol{u}'}^T \boldsymbol{u} + \frac{2Ar^{3/2}}{\sqrt{u_1'^2 + u_2'^2}}(u_1' u_2'^* - u_2' u_1'^*) \\
&\approx \frac{2Ar^{3/2}}{\sqrt{u_1'^2 + u_2'^2}}(u_1' u_2'^* - u_2' u_1'^*)
\end{aligned} \tag{46}
$$

Defining the switching function

$$
S_3(s) = u_1' u_2'^* - u_2' u_1'^* \tag{47}
$$

we ensure $Z' < 0$ by thrusting such that $A = T/m$ whenever $S_3 < 0$. The full algorithm is

1) Semimajor Axis Matching from $s_0 \leq s \leq s_i$:

$$A(s) = +T/m \quad \text{while } |\alpha(s) - \alpha^*| > \epsilon_\alpha \tag{48}$$

2) Position and Velocity Matching from $s_i \leq s \leq s_f$:

$$A(s) = \begin{cases} +T/m & \text{if } S_3(s) < 0 \\ 0 & \text{otherwise} \end{cases} \tag{49}$$

Note that the first term in Z' [before the approximation was made in Eq. (46)] depends not only on $e_\alpha \approx 0$, but also on $\boldsymbol{e}^T_{\boldsymbol{u}'} \to 0$ for $s \geq s_i$. Therefore, the product of both terms that are already close to zero will tend to zero to even a higher order of degree.

The switching scheme in Eq. (49), even though it is theoretically valid, for implementation purposes is not convenient. There is a point during the coast phase, once $\alpha \approx \alpha^*$, where the analytical harmonic oscillator solutions of both spacecraft have roughly the same amplitude. Therefore, the switching function oscillates at a constant amplitude, and it can become nonnegative for all time, $S_3(s) \geq 0$ $\forall\ s \geq s_i$. This would imply that the thrusters would never come back on, so that the chaser would never rendezvous with the target. During a coast phase, the analytical behavior of $S_3(s)$ is known (solved for in the Appendix), which lets us determine if in fact $S_3(s) \geq 0$ for all time. In this case, one possible solution is to let the thrusting acceleration be $A = -T/m$ when $S_3(s)$ is at a maximum. This will enable $S_3(s)$ to cross zero again, while ensuring that $\boldsymbol{e}_{\boldsymbol{u}} \to 0$ and $\boldsymbol{e}_{\boldsymbol{u}'} \to 0$ as time progresses. The caveat with letting $A = -T/m$ is that it results in the semimajor axis diverging from its desired value [as can be seen by the time-derivative of V in Eq. (22)] if the same control law is used [Eq. (21)]. However, a simple change in sign

$$\phi = -\lambda + \theta/2 - \sin^{-1}(K e_\alpha), \qquad K = 1/|e_{\alpha_0}| > 0 \tag{50}$$

allows for both semimajor axis convergence as well as rendezvous during this thrust phase. Therefore, the new switching scheme for the position and velocity matching section is written as

2) Position and Velocity Matching from $s_i \leq s \leq s_f$:

$$A(s) = \begin{cases} +T/m & \text{if } S_3(s) < 0; \phi \text{ given by Eq. (21)} \\ -T/m & \text{otherwise}; \phi \text{ given by Eq. (50)} \end{cases} \tag{51}$$

Another issue encountered with the switching function in Eq. (49) during the implementation is that, as the chaser gets closer to the target, $S_3(s) \to 0$ as time progresses. In fact, if at some time $s_{ii} > s_i$, $u'_1 = u'^*_1$, and $u'_2 = u'^*_2$, the switching function $S_3(s_{ii}) \equiv 0$. Once the amplitude of S_3 is within a small tolerance [$\text{amp}(S_3) \leq \epsilon_{S_3}$], any infinitesimal change in time s results in a change of sign $S_3(s)$. This leads to chattering and, therefore, full convergence is not possible to achieve. A viable and effective solution is to implement the switching function by allowing for coast arcs even when $S_3(s) < 0$, but only once the magnitude of the error in the velocity is below a specified tolerance. The continuation of the guidance scheme in Eq. (51) is written as

2i) Avoid chattering: If $\text{amp}(S_3) \leq \epsilon_{S_3}$ for $s_{ii} \leq s \leq s_f$

$$A(s) = \begin{cases} 0 & \text{if } S_3(s) \geq 0 \text{ and increasing} \\ -T/m & \text{if } S_3(s) \geq 0 \text{ and decreasing}; \phi \text{ given by Eq. (50)} \\ 0 & \text{if } S_3(s) < 0 \text{ and decreasing} \\ T/m & \text{if } S_3(s) < 0 \text{ and increasing}; \phi \text{ given by Eq. (21)} \end{cases} \tag{52}$$

The full algorithm is now given by Eqs. (48), (51), and (52). Notice that the chattering avoidance entails having the coast arcs in Eq. (52) occur until S_3 reaches either a maximum or minimum, at which point the thrusters are turned back on. A visualization of the behavior of S_3 is shown in Fig. 6d, which aids in the understanding of the thrust/coast arcs.

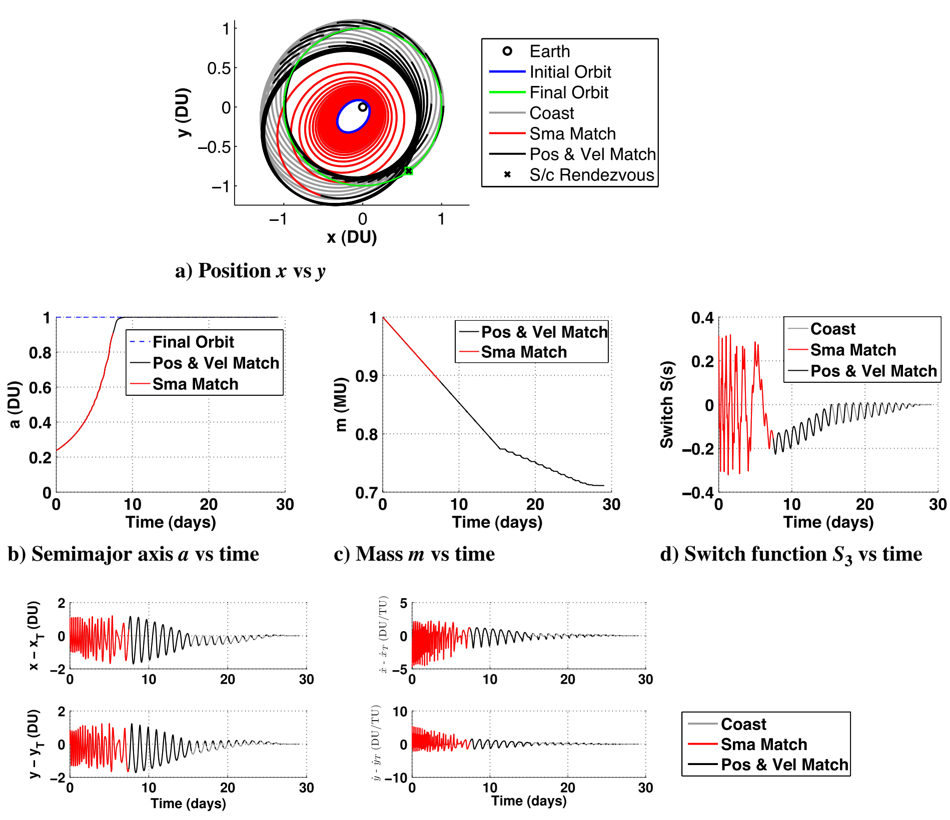

Fig. 6 Rendezvous of a chaser with a target with initial conditions given in Table 4 using $T = 5$ N and $I_{sp} = 3000$ s.

Table 4 Initial orbital elements of the chaser and target for the example in Fig. 6

Orbital elements	Target	Chaser
a_0, km	42,164	10,000
e_0	0.00	0.70
ω_0, deg	0.00	0.00
ν_0, deg	0.00	−50.00

Proposition 4: Let a spacecraft with a constant available maximum thrust T and initial mass m_0 be on a closed orbit with initial position $\boldsymbol{u}(s_0)$ and velocity $\boldsymbol{u}'(s_0)$. All solutions governed by the force model (19) with control (21) and (50), and switching function (48), (51), and (52) converge to a rendezvous solution of its target spacecraft, by matching its position $\boldsymbol{u}^*(s_f)$ and velocity $\boldsymbol{u}'^*(s_f)$.

Proof: The proof follows identically as in Proposition 2; the only difference being that the switching scheme is now given by S_3 in Eq. (47), and the coast time is analytically solved for in the Appendix. □

A rendezvous example is shown in Fig. 6, with two spacecraft (s/c) that orbit the Earth, $\mu = 398,600\ \mathrm{km}^3/\mathrm{s}^2$, with initial orbital elements given in Table 4, initial chaser mass $m_0 = 1000$ kg, a low-thrust $T = 5$ N, and $I_{\mathrm{sp}} = 3000$ s. The integration of the equations of motion is performed in dimensionless units, which are distance unit $\mathrm{DU} = a^* = 42,164$ km, mass unit $\mathrm{MU} = m_0 = 1000$ kg, and time unit TU, chosen such that $\mu = 1\ \mathrm{DU}^3/\mathrm{TU}^2$. The trajectory in x-y coordinates is shown in Fig. 6a, which has been transformed using Eq. (5) from the $\boldsymbol{u}$ results of the integration. The semimajor axis matching portion of the algorithm [Eq. (48)] is propagated until $e_\alpha \leq 0.1$, and during the second part of the algorithm, the convergence in α is met to machine precision (Fig. 6b). The switching function S_3 in Eq. (47) is plotted over time in Fig. 6d. Note that it is only once the semimajor axis has been met to the desired tolerance that it is important to know the behavior of S_3. The difference in magnitude of the position (Pos) and velocity (Vel) over time between the chaser and target are shown in Fig. 6e. Note that the target has been reached to within 10^{-4} DU of precision in position and 10^{-4} DU/TU in velocity.

VI. Conclusions

In this paper, the authors take on a new approach to the problem of orbit transfers and rendezvous by working in a transformed model to design Lyapunov-based control laws. The model they use is the classical Levi-Civita regularization transformation of the planar two-body problem. The advantage of working in these transformed coordinates is that the solution to the unperturbed equations of motion is that of a simple linear harmonic oscillator, where the frequency of oscillation is a function of a, the semimajor axis of the orbit.

The authors solve two main problems in this paper. In the first one, a closed-loop guidance scheme was designed for a coplanar orbit transfer from any initial elliptical orbit to any final specified elliptical orbit using a spacecraft with thrust–coast capabilities. The second problem solved is to achieve rendezvous with a target spacecraft, that is, to match both components of position and velocity. The convergence to the desired formation for both problems is performed in two steps. The first step involves converging the spacecraft orbit to the desired semimajor axis a^*, even though no other parameters are the desired ones at this point, by using a Lyapunov analysis that gives rise to an asymptotically stabilizing control law. Once a^* has been reached to within a specified tolerance, the second step of the algorithm involves matching the other desired orbital parameters, using the same control law as before, but with an added on/off switching mechanism for coasting during certain intervals. The other advantage of working in the Levi-Civita coordinates is that, because the analytical solution is known during the coast phases, using Lyapunov stability, it is possible to determine analytically the exact time at which the thrusters should be turned back on. The algorithms designed are robust, computationally fast, and can be used for both low- and high-thrust problems, though fuel- or time-optimality is not guaranteed. Several examples are given for various initial and final parameters as well as different engine capabilities for both the orbit transfer and rendezvous problems.

One of the powerful results of this work is that the guidance law is designed based only on matching the desired semimajor axis. With the same control law that matches the semimajor axis, the authors are able to match any desired orbit or rendezvous with a target, by adding thrust/coast arcs. However, the two convergence sections may indeed be combined virtue of selecting a different Lyapunov candidate function and redesigning the control law. This option will be studied in the authors' future work, because they are interested in designing control laws that will be closer to the fuel-optimal solution. Also, the authors would like to determine at which point during the orbit it is optimal to begin thrusting. One of the possible answers is to examine the time derivative of the candidate Lyapunov functions and determine at which point their slope is maximum, which will aid in converging to closer optimal solutions.

The next major step is to expand the orbit transfer and rendezvous algorithms to the three-dimensional model using the Kustaanheimo–Stiefel coordinate transformation, which transforms the state vector from Cartesian space into a four-dimensional space, similar to the Levi-Civita model.

Appendix: Determination of Coast-to-Thrust Switching Times

The analytical solution of the switching functions S_i, where $i = 1$, 2, 3 in Secs. IV and V are solved for here. These functions are of importance because the exact amount of coast time is found by analytically solving for the roots of the function S_i.

A1 Switching Function S_1 for Circular Orbit Transfers

The switching function S_1 defined in Eq. (30) is a function of the product of the position $\boldsymbol{u}$ [whose analytical solution is given by Eq. (17)] and the velocity $\boldsymbol{u}'$ [whose solution is found by directly taking the derivative of Eq. (17)]. Assume the frequency of oscillation is given by $\mathcal{W} = \sqrt{-E/2} = \sqrt{(\mu\alpha)/4}$ at some point in time s_0. The roots of S_1 are found by solving

$$\begin{aligned} S_1 &= u_1 u_1' + u_2 u_2' \\ &= C_1 \sin(\mathcal{W}s)\cos(\mathcal{W}s) + C_2(\cos^2(\mathcal{W}s) - \sin^2(\mathcal{W}s)) = 0 \end{aligned} \tag{A1}$$

where

$$C_1 = -\mathcal{W}(u_{1_0}^2 + u_{2_0}^2) + \frac{1}{\mathcal{W}}(u_{1_0}'^2 + u_{2_0}'^2) \quad C_2 = (u_{1_0}u_{1_0}' + u_{2_0}u_{2_0}')$$

and u_{1_0}, u_{2_0}, u_{1_0}', and u_{2_0}' are the initial conditions at s_0. The roots of the equations are given by

$$s_{\mathrm{cross}_1} = \pm\frac{1}{\mathcal{W}}\tan^{-1}\left(\frac{1}{2}\frac{\pm C_1 + \sqrt{C_1^2 + 4C_2^2}}{C_2}\right) \tag{A2}$$

which correspond to the times at which the function S_1 changes sign and therefore gives the time at which the thrusters should be turned on again after a coasting period.

A2 Switching Function S_2 for General Orbit Transfers

The roots of the switching function S_2 defined in Eq. (40) are solved for, again assuming that the frequency of oscillation is given by $\mathcal{W} = \sqrt{(\mu\alpha)/4}$ at some point in time s_0:

$$\begin{aligned} S_2 &= 2(e_x - e_x^*)u_1'u_2' + (e_y - e_y^*)(u_2'^2 - u_1'^2) \\ &= C_1 \sin(\mathcal{W}s)\cos(\mathcal{W}s) + C_2\sin^2(\mathcal{W}s) + C_3\cos^2(\mathcal{W}s) = 0 \end{aligned} \tag{A3}$$

where

$$C_1 = 2[-(e_x - e_x^*)(u_{1_0} u'_{2_0} + u'_{1_0} u_{2_0}) + (e_y - e_y^*)(u_{1_0} u'_{1_0} - u_{2_0} u'_{2_0})]\mathcal{W}$$
$$C_2 = [2(e_x - e_x^*) u_{1_0} u_{2_0} + (e_y - e_y^*)(u_{2_0}^2 - u_{1_0}^2)]\mathcal{W}^2$$
$$C_3 = [2(e_x - e_x^*) u'_{1_0} u'_{2_0} + (e_y - e_y^*)(u'^2_{2_0} - u'^2_{1_0})]$$

and e_x and e_y are defined in Eq. (34) and (35). The roots of the equations are given by

$$s_{\mathrm{cross}_2} = \pm \frac{1}{\mathcal{W}} \tan^{-1}\left(\frac{1}{2} \frac{\pm C_1 + \sqrt{C_1^2 - 4C_2C_3}}{C_2}\right) \tag{A4}$$

which correspond to the times at which the function S_2 changes sign.

A3 Switching Function S_3 for Rendezvous

The roots of the switching function S_3 in Eq. (47) are found by assuming that the chaser's semimajor axis has already converged to the target's $\alpha(s) = \alpha^*$:

$$S_3 = u'_1 u'^*_2 - u'_2 u'^*_1 = C_1 \sin(\mathcal{W}s)\cos(\mathcal{W}s) + C_2 \sin^2(\mathcal{W}s) + C_3 \cos^2(\mathcal{W}s) = 0$$

where

$$C_1 = [(u_{2_0} u'^*_{1_0} - u_{1_0} u'^*_{2_0}) + (u'_{2_0} u^*_{1_0} - u'_{1_0} u^*_{2_0})]\mathcal{W}$$
$$C_2 = [u_{1_0} u^*_{2_0} - u_{2_0} u^*_{1_0}]\mathcal{W}^2$$
$$C_3 = [u'_{1_0} u'^*_{2_0} - u'_{2_0} u'^*_{1_0}]$$

and $\boldsymbol{u}_0, \boldsymbol{u}'_0$ are the initial conditions at s_0 of the chaser and $\boldsymbol{u}^*_0, \boldsymbol{u}'^*_0$ are the initial condition of the target. The roots of the equations are given by

$$s_{\mathrm{cross}_3} = \pm \frac{1}{\mathcal{W}} \tan^{-1}\left(\frac{1}{2} \frac{\pm C_1 + \sqrt{C_1^2 - 4C_2C_3}}{C_2}\right) \tag{A5}$$

which correspond to the times at which the function S_3 changes sign and therefore gives the time at which the thrusters should be turned on again after a coasting period.

References

[1] Lawden, D. F., "Optimal Transfers Between Coplanar Elliptical Orbits," *Journal of Guidance, Control, and Dynamics*, Vol. 15, No. 3, 1992, pp. 788–791.
doi:10.2514/3.20909

[2] Edelbaum, T. N., "Optimum Power-Limited Orbit Transfer in Strong Gravity Fields," *AIAA Journal*, Vol. 3, No. 5, 1965, pp. 921–925.
doi:10.2514/3.3016

[3] Wiesel, W. E., and Alfano, S., "Optimal Many-Revolution Orbit Transfer," *Journal of Guidance, Control, and Dynamics*, Vol. 8, No. 1, 1985, pp. 155–157.
doi:10.2514/3.19952

[4] Oberle, H. J., and Taubert, K., "Existence and Multiple Solutions of the Minimum-Fuel Orbit Transfer Problem," *Journal of Optimization Theory and Applications*, Vol. 95, No. 2, 1997, pp. 243–262.
doi:10.1023/A:1022627003404

[5] Thomas, C., and Mayer, H., "Fuel-Optimal Rendezvous near a Point in General Keplerian Orbit," *Journal of Guidance, Control, and Dynamics*, Vol. 10, No. 6, 1987, pp. 567–573.

[6] Geffroy, S., and Epenoy, R., "Optimal Low-Thrust Transfers with Constraints—Generalization of Averaging Techniques," *Acta Astronautica*, Vol. 41, No. 3, 1997, pp. 133–149.
doi:10.1016/S0094-5765(97)00208-7

[7] Kechichian, J. A., "Optimal Low-Thrust Rendezvous Using Equinoctial Orbital Elements," *Acta Astronautica*, Vol. 38, No. 1, 1996, pp. 1–14.
doi:10.1016/0094-5765(95)00121-2

[8] Petropoulos, A. E., "Low-Thrust Orbit Transfers Using Candidate Lyapunov Functions with a Mechanism for Coasting," *AIAA/AAS Astrodynamics Specialist Conference*, AIAA Paper 2004-5089, Aug. 2004.

[9] Chang, D. E., Chichka, D. F., and Marsden, J. E., "Lyapunov-Based Transfer Between Elliptic Keplerian Orbits," *Discrete and Continuous Dynamical Systems-Series B*, Vol. 2, No. 1, 2002, pp. 57–67.

[10] Ilgen, M. R., "Low Thrust OTV Guidance Using Lyapunov Optimal Feedback Control Techniques," *Advances in the Astronautical Sciences*, Vol. 85, No. 2, 1993, pp. 1527–1545.

[11] Sengupta, P., and Vadali, S. R., "Satellite Orbit Transfer and Formation Reconfiguration Via an Attitude Control Analogy," *Journal of Guidance, Control, and Dynamics*, Vol. 28, No. 6, 2005, pp. 1200–1209.
doi:10.2514/1.12113

[12] Lopez, I., and McInnes, C. R., "Autonomous Rendezvous Using Artificial Potential Function Guidance," *Journal of Guidance, Control, and Dynamics*, Vol. 18, No. 2, 1995, pp. 237–241.
doi:10.2514/3.21375

[13] Zhou, B., Lin, Z., and Duan, G., "Lyapunov Differential Equation Approach to Elliptical Orbital Rendezvous with Constrained Controls," *Journal of Guidance, Control, and Dynamics*, Vol. 34, No. 2, 2011, pp. 345–358.
doi:10.2514/1.52372

[14] Aarseth, S. J., *Gravitational N-Body Simulations*, Cambridge Univ. Press, New York, 2003, pp. 51–55.

[15] Battin, R. H., *Introduction to the Mathematics and Methods of Astrodynamics*, AIAA Education Series, AIAA, Reston, VA, 1999, p. 182.

[16] Bettis, D. G., and Szebehely, V., "Treatment of Close Approaches in the Numerical Implementation Integration of the Gravitational Problem of N Bodies," *Astrophysics and Space Science*, Vol. 14, No. 1, 1971, pp. 133–150.
doi:10.1007/BF00649200

[17] Thorne, J. D., and Hall, C. D., "Minimum-Thrust Orbit Transfers Using the Kustaanheimo–Stiefel Transformation," *Journal of Guidance, Control, and Dynamics*, Vol. 20, No. 4, 1997, pp. 836–838.
doi:10.2514/2.4125

[18] Hernandez, S., Akella, M. R., and Ocampo, C. A., "Lyapunov-Based Elliptical to Circular Planar Orbit Transfers in Levi-Civita Coordinates," *Jer-Nan Juang Astrodynamics Symposium*, AAS Paper 12-616, June 2012.

[19] Hatten, N. A., "Critical Evaluation of Modern Low-Thrust Feedback-Driven Spacecraft Control Laws," M.S. Thesis, Univ. of Texas, Austin, TX, December 2012.

[20] Lu, S., and Xu, S., "Adaptive Control for Autonomous Rendezvous of Spacecraft on Elliptical Orbit," *Acta Mechanica Sinica*, Vol. 25, No. 4, 2009, pp. 539–545.
doi:10.1007/s10409-009-0235-9

[21] Stiefel, E. L., and Scheifele, G., *Linear and Regular Celestial Mechanics*, Springer–Verlag, Berlin, 1971, pp. 18–25.

[22] Edelbaum, T. N., "Optimum Low-Thrust Rendezvous and Station-Keeping," *Journal of Spacecraft and Rockets*, Vol. 40, No. 6, 2003, pp. 960–965.
doi:10.2514/2.7042

[23] Tapely, B. D., Schutz, B. E., and Born, G. H., *Statistical Orbit Determination*, Elsevier, New York, 2004, pp. 50–54.

[24] Bate, R. R., Mueller, D. D., and White, J. E., *Fundamentals of Astrodynamics*, Dover, New York, 1971, p. 62.

This article has been cited by:

1. Mayer Humi. 2017. Satellite orbits in Levi-Civita space. *Advances in Space Research* . [Crossref]
2. Sonia Hernandez, Maruthi R. Akella. 2016. Energy preserving low-thrust guidance for orbit transfers in KS variables. *Celestial Mechanics and Dynamical Astronomy* **125**:1, 107-132. [Crossref]
3. Sonia Hernandez, Maruthi R. Akella. 2015. Energy-Conserving Planar Spacecraft Motion with Constant-Thrust Acceleration. *Journal of Guidance, Control, and Dynamics* **38**:12, 2309-2323. [Abstract] [Full Text] [PDF] [PDF Plus]